Supplementary Materials for "A Ready To Use Web-Application Providing a Personalized Biopsy Schedule for Men With Low-Risk PCa Under Active Surveillance"

Anirudh Tomer, MSc[a,*], Daan Nieboer, MSc[b], Monique J. Roobol, PhD[c], Anders Bjartell, MD, PhD[d], Ewout W. Steyerberg, PhD[b,e], Dimitris Rizopoulos, PhD[a], Movember Foundations Global Action Plan Prostate Cancer Active Surveillance (GAP3) consortium[f]

[a] *Department of Biostatistics, Erasmus University Medical Center, Rotterdam, the Netherlands*
[b] *Department of Public Health, Erasmus University Medical Center, Rotterdam, the Netherlands*
[c] *Department of Urology, Erasmus University Medical Center, Rotterdam, the Netherlands*
[d] *Department of Urology, Skåne University Hospital, Malmö, Sweden*
[e] *Department of Biomedical Data Sciences, Leiden University Medical Center, Leiden, the Netherlands*
[f] *The Movember Foundations Global Action Plan Prostate Cancer Active Surveillance (GAP3) consortium members presented in Appendix F*

Appendix A. A Joint Model for the Longitudinal PSA, and Time to Gleason Upgrading

Let T_i^* denote the true time of upgrading (increase in biopsy Gleason grade group from 1 to 2 or higher) for the i-th patient included in PRIAS. Since biopsies are conducted periodically, T_i^* is observed with interval censoring $l_i < T_i^* \leq r_i$. When upgrading is observed for the patient at his latest

*Corresponding author (Anirudh Tomer): Erasmus MC, kamer flex Na-2823, PO Box 2040, 3000 CA Rotterdam, the Netherlands. Tel: +31 10 70 43393

Email addresses: a.tomer@erasmusmc.nl (Anirudh Tomer, MSc), d.nieboer@erasmusmc.nl (Daan Nieboer, MSc), m.roobol@erasmusmc.nl (Monique J. Roobol, PhD), anders.bjartell@med.lu.se (Anders Bjartell, MD, PhD), e.w.steyerberg@lumc.nl (Ewout W. Steyerberg, PhD), d.rizopoulos@erasmusmc.nl (Dimitris Rizopoulos, PhD)

biopsy time r_i, then l_i denotes the time of the second latest biopsy. Otherwise, l_i denotes the time of the latest biopsy and $r_i = \infty$. Let $\boldsymbol{y}_i$ denote his observed PSA longitudinal measurements. The observed data of all n patients is denoted by $\mathcal{D}_n = \{l_i, r_i, \boldsymbol{y}_i; i = 1, \ldots, n\}$.

In our joint model, the patient-specific PSA measurements over time are modeled using a linear mixed effects sub-model. It is given by (see Panel A, Figure 1):

$$\begin{aligned} \log_2\big\{y_i(t)+1\big\} &= m_i(t) + \varepsilon_i(t), \\ m_i(t) &= \beta_0 + b_{0i} + \sum_{k=1}^{4}(\beta_k + b_{ki})B_k\Big(\frac{t-2}{2}, \frac{\mathcal{K}-2}{2}\Big) + \beta_5 \text{age}_i, \end{aligned} \tag{1}$$

where, $m_i(t)$ denotes the measurement error free value of $\log_2(\text{PSA} + 1)$ transformed [2, 3] measurements at time t. We model it non-linearly over time using B-splines [4]. To this end, our B-spline basis function $B_k\{(t-2)/2, (\mathcal{K}-2)/2\}$ has 3 internal knots at $\mathcal{K} = \{0.5, 1.3, 3\}$ years, which are the three quartiles of the observed follow-up times. The boundary knots of the spline are at 0 and 6.3 years (95-th percentile of the observed follow-up times). We mean centered (mean 2 years) and standardized (standard deviation 2 years) the follow-up time t and the knots of the B-spline $\mathcal{K}$ during parameter estimation for better convergence. The fixed effect parameters are denoted by $\{\beta_0, \ldots, \beta_5\}$, and $\{b_{0i}, \ldots, b_{4i}\}$ are the patient specific random effects. The random effects follow a multivariate normal distribution with mean zero and variance-covariance matrix $\boldsymbol{D}$. The error $\varepsilon_i(t)$ is assumed to be t-distributed with three degrees of freedom (see Appendix B.1) and scale σ, and is independent of the random effects.

To model the impact of PSA measurements on the risk of upgrading, our joint model uses a relative risk sub-model. More specifically, the hazard of upgrading denoted as $h_i(t)$, and the cumulative risk of upgrading denoted as $R_i(t)$, at a time t are (see Panel C, Figure 1):

$$\begin{aligned} h_i(t) &= h_0(t)\exp\Big(\gamma \text{age}_i + \alpha_1 m_i(t) + \alpha_2 \frac{\mathrm{d}m_i(t)}{\mathrm{d}t}\Big), \\ R_i(t) &= \exp\Big\{-\int_0^t h_i(s)\mathrm{d}s\Big\}, \end{aligned} \tag{2}$$

where, γ is the parameter for the effect of age. The impact of PSA on the hazard of upgrading is modeled in two ways, namely the impact of the error

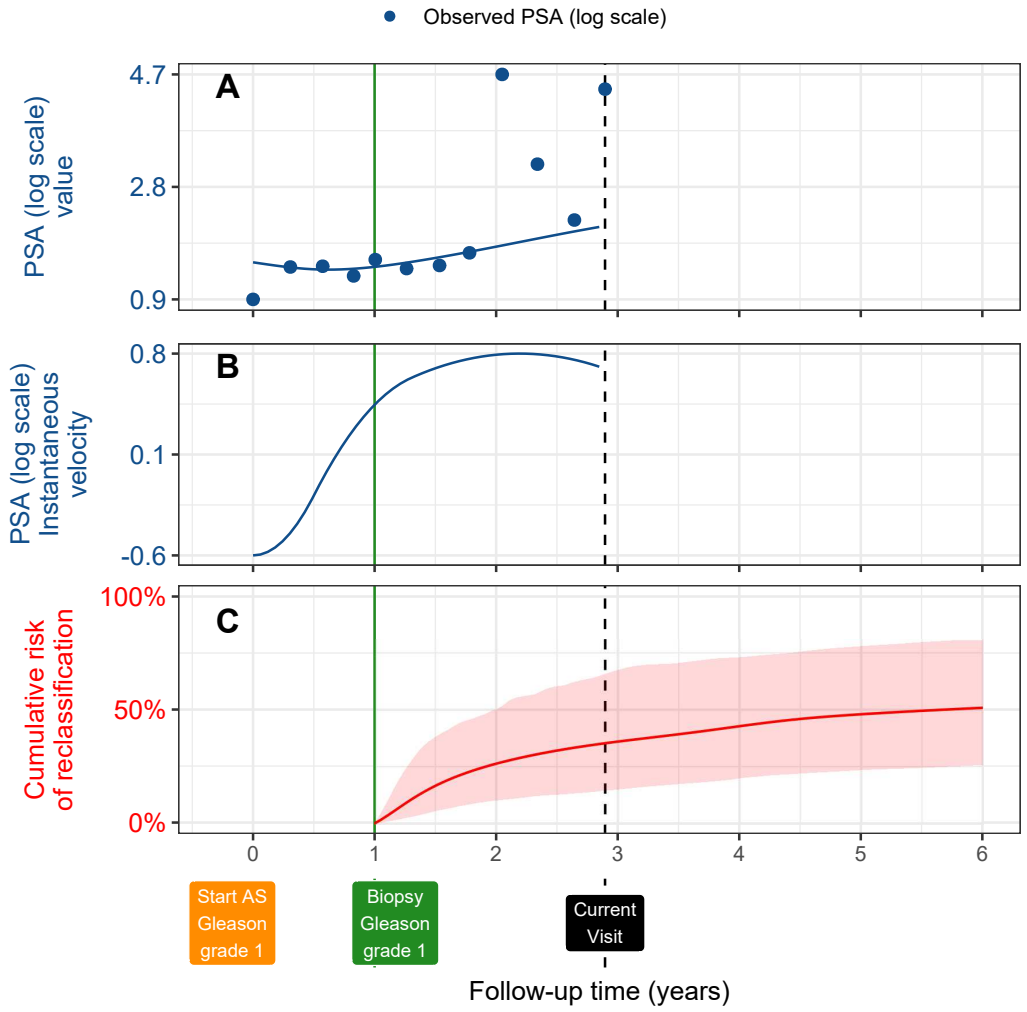

Figure 1: **Illustration of the joint model on a real PRIAS dataset patient**. **Panel A:** Observed (blue dots) and fitted PSA (solid blue line) measurements, log-transformed. **Panel B:** Estimated instantaneous velocity of PSA (log-transformed). **Panel C**: Predicted cumulative-risk of upgrading (95% credible interval shaded). Upgrading is defined as increase in Gleason grade group [1] from grade group 1 to 2 or higher. This risk of upgrading is available starting from the time of the latest negative biopsy (vertical green line at year 1 of follow-up). Joint model estimated it by combining the fitted PSA value and velocity (both on log scale of PSA) and time of latest negative biopsy. Black dashed line at year 4 denotes time of current visit.

free underlying PSA value $m_i(t)$ (see Panel A, Figure 1), and the impact of the underlying PSA velocity $\mathrm{d}m_i(t)/\mathrm{d}t$ (see Panel B, Figure 1). The corresponding parameters are α_1 and α_2, respectively. Lastly, $h_0(t)$ is the baseline hazard at time t, and is modeled flexibly using P-splines [5]. More specifically:

$$\log h_0(t) = \gamma_{h_0,0} + \sum_{q=1}^{Q} \gamma_{h_0,q} B_q(t, \boldsymbol{v}),$$

where $B_q(t, \boldsymbol{v})$ denotes the q-th basis function of a B-spline with knots $\boldsymbol{v} = v_1, \ldots, v_Q$ and vector of spline coefficients γ_{h_0}. To avoid choosing the number and position of knots in the spline, a relatively high number of knots (e.g., 15 to 20) are chosen and the corresponding B-spline regression coefficients γ_{h_0} are penalized using a differences penalty [5].

We estimate the parameters of the joint model using Markov chain Monte Carlo (MCMC) methods under the Bayesian framework. Let $\boldsymbol{\theta}$ denote the vector of all of the parameters of the joint model. The joint model postulates that given the random effects, the time of upgrading, and the PSA measurements taken over time are all mutually independent. Under this assumption the posterior distribution of the parameters is given by:

$$\begin{aligned} p(\boldsymbol{\theta}, \boldsymbol{b} \mid \mathcal{D}_n) &\propto \prod_{i=1}^{n} p(l_i, r_i, \boldsymbol{y}_i, \mid \boldsymbol{b}_i, \boldsymbol{\theta}) p(\boldsymbol{b}_i \mid \boldsymbol{\theta}) p(\boldsymbol{\theta}) \\ &\propto \prod_{i=1}^{n} p(l_i, r_i \mid \boldsymbol{b}_i, \boldsymbol{\theta}) p(\boldsymbol{y}_i \mid \boldsymbol{b}_i, \boldsymbol{\theta}) p(\boldsymbol{b}_i \mid \boldsymbol{\theta}) p(\boldsymbol{\theta}), \\ p(\boldsymbol{b}_i \mid \boldsymbol{\theta}) &= \frac{1}{\sqrt{(2\pi)^q \det(\boldsymbol{D})}} \exp\Big\{ -\frac{1}{2} (\boldsymbol{b}_i^T \boldsymbol{D}^{-1} \boldsymbol{b}_i) \Big\}, \end{aligned}$$

where, the likelihood contribution of the PSA outcome, conditional on the random effects is:

$$p(\boldsymbol{y}_i \mid \boldsymbol{b}_i, \boldsymbol{\theta}) = \frac{1}{\left(\sqrt{2\pi\sigma^2}\right)^{n_i}} \exp\left\{ -\frac{\sum_{j=1}^{n_i} \left(y_{ij} - m_{ij}\right)^2}{2\sigma^2} \right\},$$

where n_i is the number of PSA measurements of the i-th patient. The likelihood contribution of the time of upgrading outcome is given by:

$$p(l_i, r_i \mid \boldsymbol{b}_i, \boldsymbol{\theta}) = \exp\Big\{ -\int_0^{l_i} h_i(s) \mathrm{d}s \Big\} - \exp\Big\{ -\int_0^{r_i} h_i(s) \mathrm{d}s \Big\}. \qquad (3)$$

The integrals in (3) do not have a closed-form solution, and therefore we use a 15-point Gauss-Kronrod quadrature rule to approximate them.

We use independent normal priors with zero mean and variance 100 for the fixed effects $\{\beta_0, \ldots, \beta_5\}$, and inverse Gamma prior with shape and rate both equal to 0.01 for the parameter σ^2. For the variance-covariance matrix $\boldsymbol{D}$ of the random effects we take inverse Wishart prior with an identity scale matrix and degrees of freedom equal to 5 (number of random effects). For the relative risk model's parameter γ and the association parameters α_1, α_2, we use independent normal priors with zero mean and variance 100.

Appendix A.1. Assumption of t-distributed (df=3) Error Terms

With regards to the choice of the distribution for the error term ε for the PSA measurements (see Equation 1), we attempted fitting multiple joint models differing in error distribution, namely t-distribution with three, and four degrees of freedom, and a normal distribution for the error term. However, the model assumption for the error term were best met by the model with t-distribution having three degrees of freedom. The quantile-quantile plot of subject-specific residuals for the corresponding model in Panel A of Figure 2, shows that the assumption of t-distributed (df=3) errors is reasonably met by the fitted model.

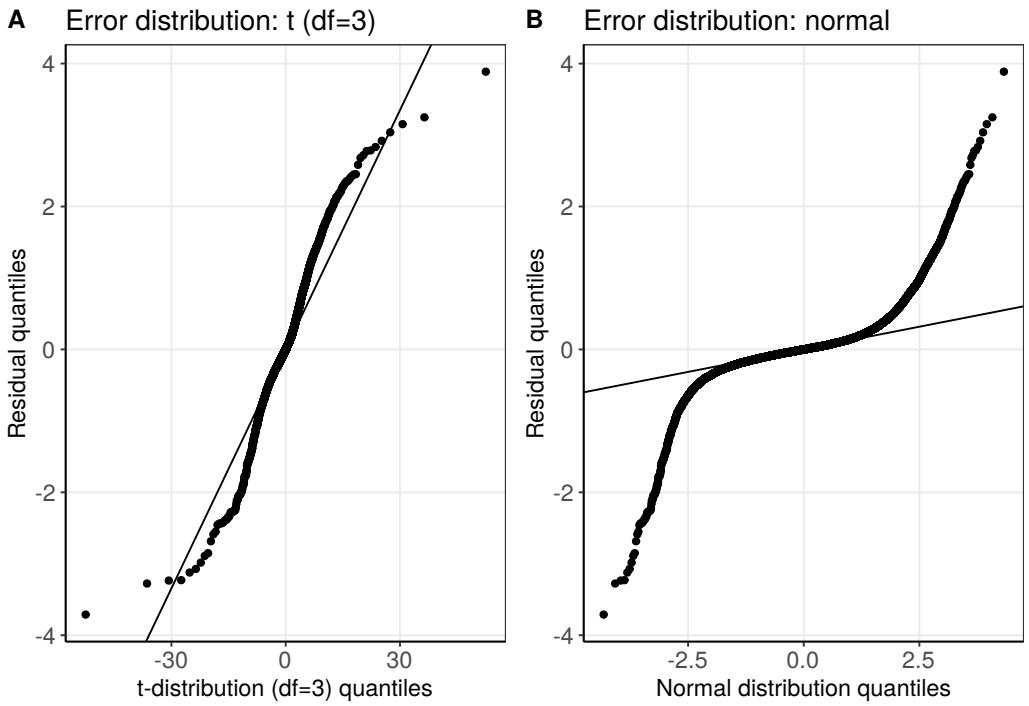

Figure 2: **Quantile-quantile plot** of subject-specific PSA residuals from two different joint models fitted to the PRIAS dataset. **Panel A**: model assuming a t-distribution (df=3) for the error term ε (see Equation 1). **Panel B**: model assuming a normal distribution for the error term ε.

Table 1: **Estimated variance-covariance matrix $\boldsymbol{D}$** of the random effects $\boldsymbol{b} = (b_0, b_1, b_2, b_3, b_4)$ from the joint model fitted to the PRIAS dataset. The variances of the random effects are highlighted along the diagonal of the variance-covariance matrix.

Random Effects	b_0	b_1	b_2	b_3	b_4
b_0	**0.229**	0.030	0.023	0.073	0.007
b_1	0.030	**0.149**	0.098	0.171	0.085
b_2	0.023	0.098	**0.276**	0.335	0.236
b_3	0.073	0.171	0.335	**0.560**	0.359
b_4	0.007	0.085	0.236	0.359	**0.351**

Table 2: **Parameters of the longitudinal sub-model**: Estimated mean and 95% credible interval for parameters in Equation (1).

Variable	Mean	Std. Dev	2.5%	97.5%	P
Intercept	2.129	0.060	2.009	2.244	<0.001
Age	0.008	0.001	0.007	0.010	<0.001
Spline: [0.0, 0.5] years	0.063	0.007	0.051	0.075	<0.001
Spline: [0.5, 1.3] years	0.196	0.010	0.177	0.217	<0.001
Spline: [1.3, 3.0] years	0.244	0.014	0.217	0.272	<0.001
Spline: [3.0, 6.3] years	0.382	0.014	0.356	0.410	<0.001
σ	0.139	0.001	0.138	0.140	

Appendix A.2. Results

The joint model was fitted using the R package **JMbayes** [8]. This package utilizes the Bayesian methodology to estimate model parameters. The corresponding posterior parameter estimates are shown in Table 2 (longitudinal sub-model for PSA outcome) and Table 3 (relative risk sub-model). The parameter estimates for the variance-covariance matrix $\boldsymbol{D}$ from the longitudinal sub-model for PSA are shown in the following Table 1:

For the PSA mixed effects sub-model parameter estimates (see Equation 1), in Table 2 we can see that the age of the patient trivially affects the baseline $\log_2(\text{PSA} + 1)$ measurement. Since the longitudinal evolution of $\log_2(\text{PSA} + 1)$ measurements is modeled with non-linear terms, the interpretation of the coefficients corresponding to time is not straightforward. In lieu of the interpretation, in Figure 4 we present plots of observed versus fitted PSA profiles for nine randomly selected patients.

For the relative risk sub-model (see Equation 2), the parameter estimates in Table 3 show that $\log_2(\text{PSA} + 1)$ velocity and age of the patient were significantly associated with the hazard of upgrading.

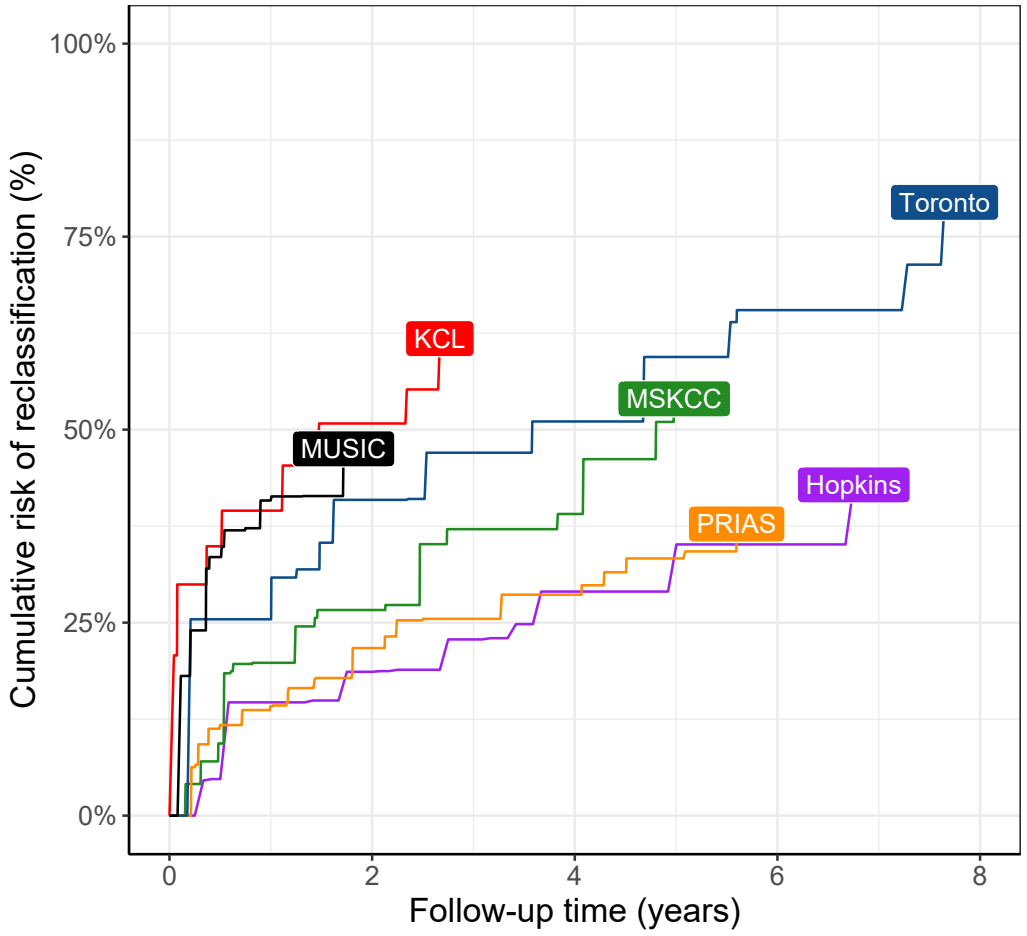

Figure 3: **Nonparametric estimate [6] of cumulative risk of upgrading** in the world's largest AS cohort PRIAS, and largest five AS cohorts from the GAP3 database [7]. Abbreviations are *Hopkins*: Johns Hopkins Active Surveillance, *PRIAS*: Prostate Cancer International Active Surveillance, *Toronto*: University of Toronto Active Surveillance, *MSKCC*: Memorial Sloan Kettering Cancer Center Active Surveillance, *KCL*: King's College London Active Surveillance, *MUSIC*: Michigan Urological Surgery Improvement Collaborative AS.

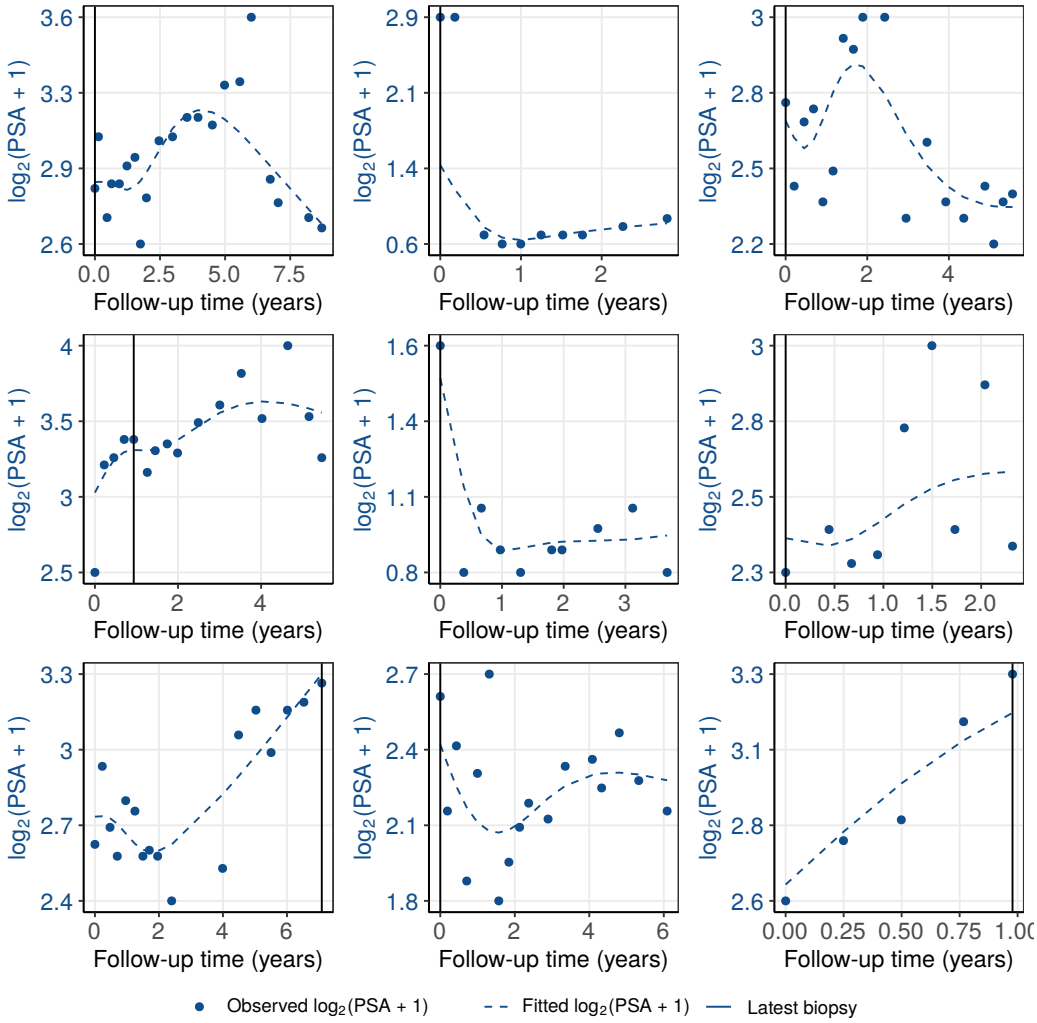

Figure 4: **Fitted versus observed** $\log_2(\mathbf{PSA}+1)$ **profiles** for nine randomly selected PRIAS patients. The fitted profiles utilize information from the observed PSA measurements, and time of the latest biopsy.

Table 3: **Parameters of the relative risk sub-model**: Estimated mean and 95% credible interval for the parameters in Equation (2).

Variable	Mean	Std. Dev	2.5%	97.5%	P
Age	0.037	0.006	0.025	0.049	<0.001
Fitted $\log_2(\text{PSA}+1)$ value	-0.012	0.076	-0.164	0.135	0.856
Fitted $\log_2(\text{PSA}+1)$ velocity	2.266	0.299	1.613	2.767	<0.001

Table 4: **Hazard ratio and 95% credible interval (CI) for upgrading**: Variables are on different scale and hence we compare an increase in the variables of relative risk sub-model from their 25-th percentile (P_{25}) to their 75-th percentile (P_{75}). Except for age, quartiles for all other variables are based on their fitted values obtained from the joint model fitted to the PRIAS dataset.

Variable	P_{25}	P_{75}	Hazard ratio [95% CI]
Age	61	71	1.455 [1.285, 1.631]
Fitted $\log_2(\text{PSA}+1)$ value	2.360	3.078	0.991 [0.889, 1.102]
Fitted $\log_2(\text{PSA}+1)$ velocity	-0.085	0.308	2.433 [1.883, 2.962]

Table 5: **Effect of $\log_2(\text{PSA}+1)$ value and velocity on hazard of upgrading in different cohorts**. We fitted separate joint models for each of the five GAP3 validation cohorts. The specification of these joint models was same as that of the model for PRIAS. Two important parameters of the relative-risk sub-model, namely, the $\log_2(\text{PSA}+1)$ value and velocity differ between the cohorts. The mean estimate of these parameters with 95% credible interval in brackets is given below. Strongest average effect of PSA velocity is in PRIAS cohort, whereas the weakest is in KCL cohort. The strongest average effect of PSA value is in the Toronto cohort whereas the weakest is in PRIAS cohort.

Cohort	Fitted $\log_2(\text{PSA}+1)$ value	Fitted $\log_2(\text{PSA}+1)$ velocity
PRIAS	-0.012 [-0.164, 0.135]	2.266 [1.613, 2.767]
Hopkins	0.061 [-0.323, 0.329]	1.839 [0.761, 4.378]
MSKCC	0.336 [0.081, 0.583]	1.122 [0.421, 1.980]
Toronto	0.572 [0.347, 0.794]	0.943 [0.464, 1.554]
MUSIC	0.441 [0.092, 0.767]	0.029 [-0.552, 0.512]
KCL	0.194 [-0.104, 0.540]	0.840 [-0.087, 1.665]

It is important to note that since age, and $\log_2(\text{PSA}+1)$ value and velocity are all measured on different scales, a comparison between the corresponding parameter estimates is not easy. To this end, in Table 4, we present the hazard ratio of upgrading, for an increase in the aforementioned variables from their 25-th to the 75-th percentile. For example, an increase in fitted $\log_2(\text{PSA}+1)$ velocity from -0.085 to 0.308 (fitted 25-th and 75-th percentiles) corresponds to a hazard ratio of 2.433. The interpretation for the rest is similar.

Appendix B. Risk Predictions for Upgrading

Let us assume a new patient j, for whom we need to estimate the risk of upgrading. Let his current follow-up visit time be s, latest time of biopsy be t, observed vector PSA measurements be $\mathcal{Y}_j(s)$. The combined information from the observed data about the time of upgrading, is given by the following posterior predictive distribution $g(T_j^*)$ of his time T_j^* of upgrading:

$$\begin{aligned} g(T_j^*) &= p\big\{T_j^* \mid T_j^* > t, \mathcal{Y}_j(s), \mathcal{D}_n\big\} \\ &= \int\int p\big(T_j^* \mid T_j^* > t, \boldsymbol{b}_j, \boldsymbol{\theta}\big) \\ &\quad \times p\big\{\boldsymbol{b}_j \mid T_j^* > t, \mathcal{Y}_j(s), \boldsymbol{\theta}\big\} p\big(\boldsymbol{\theta} \mid \mathcal{D}_n\big) \mathrm{d}\boldsymbol{b}_j \mathrm{d}\boldsymbol{\theta}. \end{aligned}$$

The distribution $g(T_j^*)$ depends not only depends on the observed data of the patient $T_j^* > t, \mathcal{Y}_j(s)$, but also depends on the information from the PRIAS dataset $\mathcal{D}_n$. To this the the posterior distribution of random effects $\boldsymbol{b}_j$ and posterior distribution of the vector of all parameters $\boldsymbol{\theta}$ are utilized, respectively. The distribution $g(T_j^*)$ can be estimated as detailed in Rizopoulos et al. [9]. Since, majority of the prostate cancer patients may not obtain upgrading in the current follow-up period of PRIAS (thirteen years), $g(T_j^*)$ can only be estimated for a currently limited follow-up period.

The cumulative risk of upgrading can be derived from $g(T_j^*)$ as given in [9]. It is given by:

$$R_j(u \mid t, s) = \Pr\big\{T_j^* > u \mid T_j^* > t, \mathcal{Y}_j(s), \mathcal{D}_n\big\}, \quad u \geq t. \tag{4}$$

The personalized risk profile of the patient (see Panel C, Figure 5) updates as more data is gathered over follow-up visits.

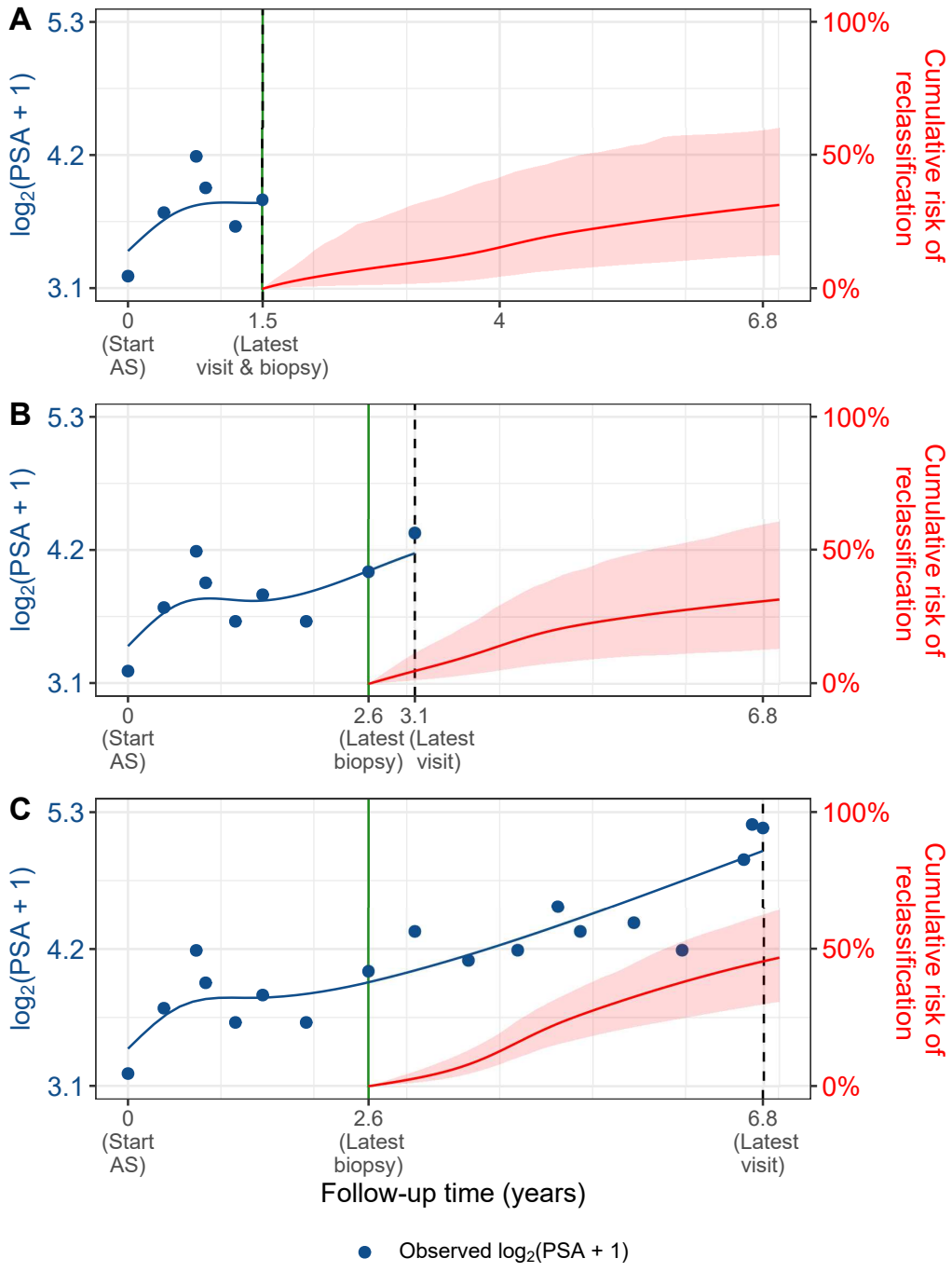

Figure 5: **Cumulative risk of (upgrading) changing dynamically over follow-up** as more patient data is gathered. The three **Panels A,B and C:** are ordered by the time of the latest visit (dashed vertical black line) of a new patient. At each of the latest follow-up visits, we combine the accumulated PSA measurements (shown in blue), and latest time of negative biopsy (solid vertical green line) to obtain the updated cumulative risk profile (shown in red) of the patient.

Appendix B.1. Validation of Risk Predictions

We wanted to check the usefulness of our model for not only the PRIAS patients but also for patients from other cohorts. To this end, we validated our model in the PRIAS dataset (internal validation) and in largest five cohorts from the GAP3 database [7]. These are the University of Toronto AS (Toronto), Johns Hopkins AS (Hopkins), Memorial Sloan Kettering Cancer Center AS (MSKCC), King's College London AS (KCL), and Michigan Urological Surgery Improvement Collaborative AS (MUSIC).

Calibration-in-the-large We first assessed calibration-in-the-large [10] of our model in the aforementioned cohorts. To this end, we used our model to predict the cumulative risk of upgrading for each patient given their PSA measurements and biopsy results. We then averaged the resulting profiles of cumulative risk of upgrading. Subsequently we compared the averaged cumulative-risk profile with a non-parametric estimate [6] of the cumulative risk of upgrading in each of the cohorts. The results are shown in Panel A of Figure 6. We can see that our model's calibration is fine only in PRIAS and Hopkins cohorts. To improve our model's calibration in KCL, MUSIC, Toronto, and MSKCC cohorts, we recalibrated the baseline hazard of the joint model fitted to the PRIAS dataset, individually for each of these cohorts. More specifically, given the data of an external cohort $\mathcal{D}_n^c$, where c denotes the cohort, the recalibrated parameters $\boldsymbol{\gamma}_{h0}^c$ (Appendix A) of the log baseline hazard are given by:

$$p(\boldsymbol{\gamma}_{h0}^c \mid \mathcal{D}_n^c, \boldsymbol{b^c}, \boldsymbol{\theta}) \propto \prod_{i=1}^{n^c} p(l_i^c, r_i^c \mid \boldsymbol{b_i^c}, \boldsymbol{\theta}) p(\boldsymbol{\gamma}_{h0}^c) \tag{5}$$

where n^c are the number of patients in the c-th cohort and $\boldsymbol{\theta}$ are the parameters of the joint model fitted to the PRIAS dataset. The interval in which upgrading is observed for the $i-th$ patient is given by l_i^c, r_i^c, with $r_i^c = \infty$ for right censored patients. The symbol $\boldsymbol{b_i^c}$ denotes patient-specific random effects (Appendix A). The random effects are obtained using the joint model fitted to the PRIAS dataset prior to recalibration. We re-evaluated the calibration-in-the-large of our model after the recalibration of the baseline hazard individually for each cohort. The improved calibration-in-the-large is shown in Panel B of Figure 6.

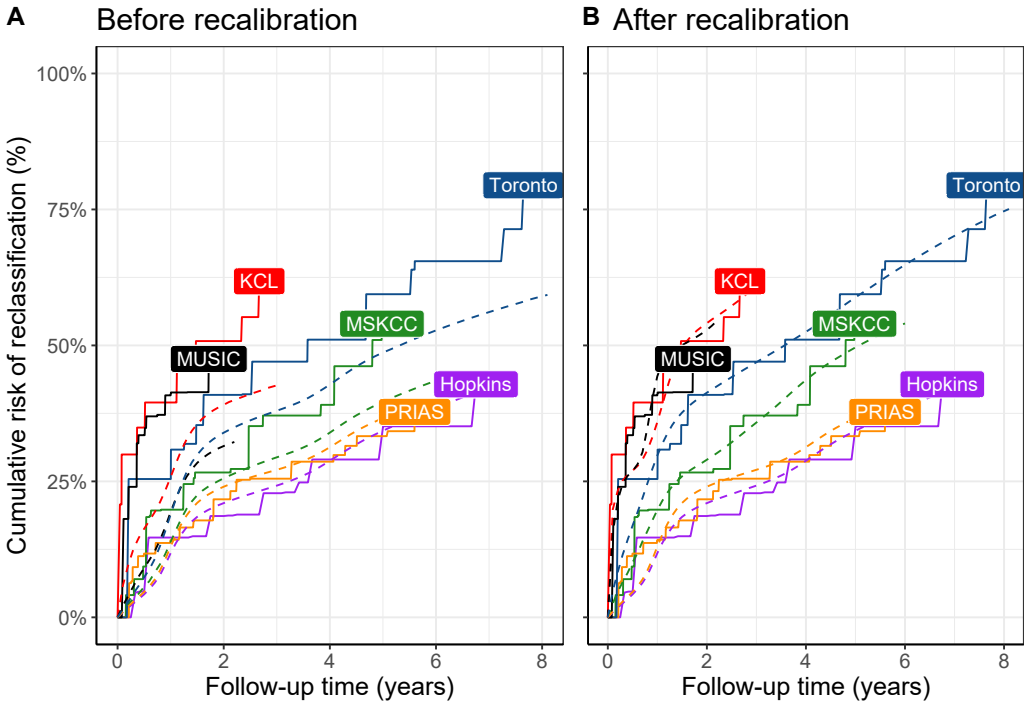

Figure 6: **Calibration-in-the-large of our model:**. In **Panel A** we can see that our model is not well calibrated for use in KCL, MUSIC, Toronto and MSKCC. In **Panel B** we can see that calibration of model predictions improved in KCL, MUSIC, Toronto and MSKCC cohorts after recalibrating our model. Recalibration was not necessary for Hopkins cohort. Full names of Cohorts are *PRIAS*: Prostate Cancer International Active Surveillance, *Toronto*: University of Toronto Active Surveillance, *Hopkins*: Johns Hopkins Active Surveillance, *MSKCC*: Memorial Sloan Kettering Cancer Center Active Surveillance, *KCL*: King's College London Active Surveillance, *MUSIC*: Michigan Urological Surgery Improvement Collaborative Active Surveillance.

Recalibrated PRIAS Model Versus Individual Joint Models For Each Cohort We wanted to check if our recalibrated PRIAS model performed as good as a new joint model that could be fitted to the external cohorts. To this end, we predicted cumulative-risk of upgrading for each patient from each cohort using two sets of models, namely the recalibrated PRIAS model for each cohort, and a new joint model fitted to each cohort. The difference in predicted cumulative-risk of upgrading from these models is shown in Figure 7. We can see that the difference is smaller in those cohorts in which the effects of $\log_2(\text{PSA}+1)$ value and velocity were similar to that of PRIAS (Table 5). For example, the Hopkins cohort had parameter estimates similar to that of PRIAS and consequently the difference in predicted risks for this cohort is smallest. The opposite of this phenomenon holds true for the MUSIC and KCL cohorts.

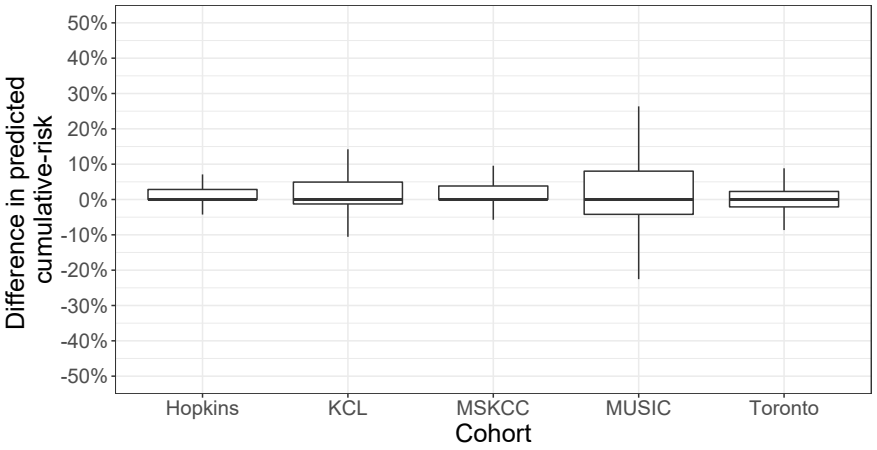

Figure 7: **Comparison of predictions from recalibrated PRIAS model with individual joint models fitted to external cohorts:** On Y-axis we show the difference between predicted cumulative-risk of upgrading for individual patients using two models, namely the recalibrated PRIAS model for each cohort, and individual joint model fitted to each cohort. The figure shows that the difference is smaller in those cohorts in which the effects of $\log_2(\text{PSA}+1)$ value and velocity were similar to that of PRIAS (Table 5). Full names of Cohorts are *PRIAS*: Prostate Cancer International Active Surveillance, *Toronto*: University of Toronto Active Surveillance, *Hopkins*: Johns Hopkins Active Surveillance, *MSKCC*: Memorial Sloan Kettering Cancer Center Active Surveillance, *KCL*: King's College London Active Surveillance, *MUSIC*: Michigan Urological Surgery Improvement Collaborative Active Surveillance.

Validation of Dynamic Cumulative-Risk Predictions As shown in Figure 5 the cumulative-risk predictions from the joint model are dynamic in nature. That is, they update as more data becomes available over time. Consequently, the discrimination and calibration of the joint model also depends on the available data. We assessed these two measures dynamically in the PRIAS cohort (interval validation) and in the largest five external cohorts that are part of the GAP3 database. For discrimination we utilized the time-varying area under the receiver operating characteristic curve or time-varying AUC [9]. For time-varying calibration we assessed the mean absolute prediction error or MAPE [9]. The AUC indicates how well the model discriminates between patients who experience upgrading and those do not. The MAPE indicates how accurately the model predicts upgrading. Both AUC and MAPE are restricted to $[0, 1]$. However, it is preferred that AUC > 0.5 because an AUC ≤ 0.5 indicates that the model performs worse than random discrimination. Ideally MAPE should be 0.

We calculate AUC and MAPE in a time-dependent manner. More specifically, given the time of latest biopsy t, and history of PSA measurements up to time s, we calculate AUC and MAPE for a medically relevant time frame $(t, s]$, within which the occurrence of upgrading is of interest. In the case of prostate cancer, at any point in time s it is of interest to identify patients who may have experienced upgrading in the last one year $(s - 1, s]$. That is we set $t = s - 1$. We then calculate AUC and MAPE at a gap of every six months (follow-up schedule of PRIAS). That is, $s\epsilon\{1, 1.5, \ldots\}$ years. To obtain reliable estimates of AUC and MAPE, in each cohort we restrict s to a maximum time point $s_{\max}$, such that there are at least 10 patients who experience upgrading after $s_{\max}$. This maximum time point $s_{\max}$ differs between cohorts, and is given in Table 6.

The results for estimates of AUC and MAPE are summarized in Figure 8, and in Table 7 to Table 12. Results are based on the recalibrated PRIAS model for the GAP3 cohorts. The results show that AUC remains more or less constant in all cohorts as more data becomes available for patients. The AUC obtains a moderate value, roughly between 0.5 and 0.7 for all cohorts. On the other hand, MAPE reduces by a big margin after year two of follow-up. This could be because of two reasons. Firstly, MAPE at year one is based only on four PSA measurements gathered in first year of follow-up, whereas after year two number of PSA measurements increase. Secondly, patients in year one consist of two sub-populations, namely patients with a correct Gleason grade 1 at the time of inclusion in AS, and patients who probably

Table 6: **Maximum follow-up period up to which we can reliably predict risk of upgrading**. In each cohort, this time point is chosen such that there are at least 10 patients who experience upgrading after this time point. Full names of Cohorts are *PRIAS*: Prostate Cancer International Active Surveillance, *Toronto*: University of Toronto Active Surveillance, *Hopkins*: Johns Hopkins Active Surveillance, *MSKCC*: Memorial Sloan Kettering Cancer Center Active Surveillance, *KCL*: King's College London Active Surveillance, *MUSIC*: Michigan Urological Surgery Improvement Collaborative Active Surveillance.

Cohort	Maximum Prediction Time (years)
PRIAS	6
KCL	3
MUSIC	2
Toronto	8
MSKCC	6
Hopkins	7

had Gleason grade 2 at inclusion but were misclassified by the urologist as Gleason grade 1 patients. To remedy this problem, a biopsy for all patients at year one is commonly recommended in all AS programs [11].

Table 7: **Internal validation of predictions of upgrading in PRIAS cohort**. The area under the receiver operating characteristic curve or AUC (measure of discrimination) and mean absolute prediction error or MAPE (measure of calibration) are calculated over the follow-up period at a gap of 6 months. In addition bootstrapped 95% confidence intervals (CI) are also presented.

Follow-up period (years)	AUC (95% CI)	MAPE (95%CI)
0.0 to 1.0	0.652 [0.611, 0.690]	0.220 [0.214, 0.227]
0.5 to 1.5	0.657 [0.641, 0.673]	0.260 [0.254, 0.265]
1.0 to 2.0	0.661 [0.647, 0.678]	0.187 [0.183, 0.191]
1.5 to 2.5	0.647 [0.596, 0.688]	0.129 [0.122, 0.140]
2.0 to 3.0	0.683 [0.642, 0.723]	0.135 [0.125, 0.146]
2.5 to 3.5	0.692 [0.632, 0.748]	0.118 [0.111, 0.128]
3.0 to 4.0	0.657 [0.603, 0.709]	0.086 [0.080, 0.092]
3.5 to 4.5	0.623 [0.582, 0.660]	0.111 [0.105, 0.116]
4.0 to 5.0	0.619 [0.582, 0.654]	0.126 [0.118, 0.131]
4.5 to 5.5	0.624 [0.537, 0.711]	0.119 [0.103, 0.135]
5.0 to 6.0	0.639 [0.582, 0.696]	0.121 [0.103, 0.138]

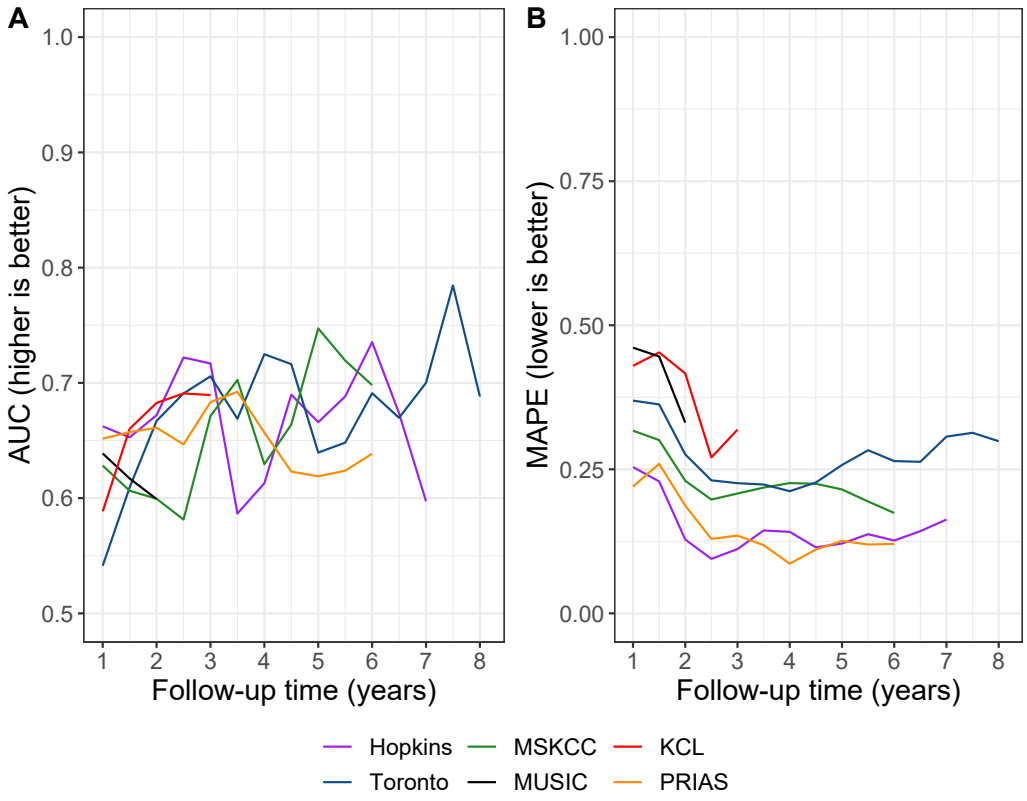

Figure 8: **Validation of Dynamic Cumulative-Risk Predictions**. In **Panel A** we can see that the time dependent area under the receiver operating characteristic curve or AUC (measure of discrimination) is above 0.5 in PRIAS (internal validation), and in Toronto, Hopkins, MSKCC, KCL, and MUSIC AS cohorts (external validation). In **Panel B** we can see that the time dependent root mean squared prediction error or MAPE (measure of calibration) is similar for PRIAS and Hopkins cohorts. The bootstrapped 95% confidence interval for these estimates are presented in Table 7 to Table 11. Full names of Cohorts are *PRIAS*: Prostate Cancer International Active Surveillance, *Toronto*: University of Toronto Active Surveillance, *Hopkins*: Johns Hopkins Active Surveillance, *MSKCC*: Memorial Sloan Kettering Cancer Center Active Surveillance, *KCL*: King's College London Active Surveillance, *MUSIC*: Michigan Urological Surgery Improvement Collaborative Active Surveillance.

Table 8: **External validation of predictions of upgrading in University of Toronto Active Surveillance cohort**. The area under the receiver operating characteristic curve or AUC (measure of discrimination) and mean absolute prediction error or MAPE (measure of calibration) are calculated over the follow-up period at a gap of 6 months. In addition bootstrapped 95% confidence intervals (CI) are also presented.

Follow-up period (years)	AUC (95% CI)	MAPE (95%CI)
0.0 to 1.0	0.541 [0.470, 0.621]	0.369 [0.352, 0.381]
0.5 to 1.5	0.609 [0.547, 0.661]	0.363 [0.348, 0.376]
1.0 to 2.0	0.667 [0.634, 0.712]	0.276 [0.259, 0.296]
1.5 to 2.5	0.691 [0.651, 0.730]	0.231 [0.205, 0.254]
2.0 to 3.0	0.706 [0.637, 0.762]	0.226 [0.196, 0.260]
2.5 to 3.5	0.669 [0.586, 0.741]	0.224 [0.195, 0.258]
3.0 to 4.0	0.725 [0.649, 0.806]	0.212 [0.184, 0.238]
3.5 to 4.5	0.716 [0.642, 0.793]	0.227 [0.206, 0.258]
4.0 to 5.0	0.640 [0.579, 0.717]	0.257 [0.222, 0.312]
4.5 to 5.5	0.648 [0.579, 0.740]	0.283 [0.247, 0.326]
5.0 to 6.0	0.691 [0.608, 0.793]	0.264 [0.232, 0.302]
5.5 to 6.5	0.670 [0.543, 0.776]	0.263 [0.227, 0.307]
6.0 to 7.0	0.700 [0.544, 0.851]	0.307 [0.258, 0.363]
6.5 to 7.5	0.785 [0.640, 0.866]	0.313 [0.272, 0.360]
7.0 to 8.0	0.688 [0.532, 0.786]	0.299 [0.249, 0.361]

Table 9: **External validation of predictions of upgrading in Johns Hopkins Active Surveillance cohort**. The area under the receiver operating characteristic curve or AUC (measure of discrimination) and mean absolute prediction error or MAPE (measure of calibration) are calculated over the follow-up period at a gap of 6 months. In addition bootstrapped 95% confidence intervals (CI) are also presented.

Follow-up period (years)	AUC (95% CI)	MAPE (95%CI)
0.0 to 1.0	0.662 [0.586, 0.715]	0.254 [0.245, 0.265]
0.5 to 1.5	0.653 [0.603, 0.707]	0.229 [0.219, 0.240]
1.0 to 2.0	0.672 [0.604, 0.744]	0.128 [0.115, 0.141]
1.5 to 2.5	0.722 [0.652, 0.792]	0.095 [0.081, 0.111]
2.0 to 3.0	0.717 [0.638, 0.777]	0.112 [0.100, 0.123]
2.5 to 3.5	0.587 [0.493, 0.704]	0.144 [0.129, 0.154]
3.0 to 4.0	0.613 [0.486, 0.742]	0.141 [0.126, 0.156]
3.5 to 4.5	0.690 [0.594, 0.783]	0.115 [0.100, 0.133]
4.0 to 5.0	0.666 [0.572, 0.754]	0.121 [0.104, 0.147]
4.5 to 5.5	0.688 [0.519, 0.779]	0.137 [0.119, 0.161]
5.0 to 6.0	0.735 [0.676, 0.820]	0.126 [0.102, 0.152]
5.5 to 6.5	0.674 [0.581, 0.765]	0.143 [0.121, 0.172]
6.0 to 7.0	0.597 [0.472, 0.712]	0.163 [0.126, 0.195]

Table 10: **External validation of predictions of upgrading in Memorial Sloan Kettering Cancer Center Active Surveillance cohort**. The area under the receiver operating characteristic curve or AUC (measure of discrimination) and mean absolute prediction error or MAPE (measure of calibration) are calculated over the follow-up period at a gap of 6 months. In addition bootstrapped 95% confidence intervals (CI) are also presented.

Follow-up period (years)	AUC (95% CI)	MAPE (95%CI)
0.0 to 1.0	0.628 [0.577, 0.688]	0.317 [0.316, 0.318]
0.5 to 1.5	0.606 [0.532, 0.657]	0.301 [0.290, 0.311]
1.0 to 2.0	0.599 [0.518, 0.671]	0.230 [0.207, 0.256]
1.5 to 2.5	0.581 [0.504, 0.663]	0.198 [0.168, 0.235]
2.0 to 3.0	0.671 [0.599, 0.741]	0.208 [0.182, 0.232]
2.5 to 3.5	0.703 [0.610, 0.777]	0.218 [0.197, 0.246]
3.0 to 4.0	0.629 [0.499, 0.706]	0.226 [0.194, 0.259]
3.5 to 4.5	0.664 [0.589, 0.756]	0.225 [0.199, 0.262]
4.0 to 5.0	0.747 [0.642, 0.841]	0.215 [0.188, 0.247]
4.5 to 5.5	0.719 [0.597, 0.852]	0.194 [0.165, 0.232]
5.0 to 6.0	0.698 [0.565, 0.792]	0.174 [0.136, 0.227]

Table 11: **External validation of predictions of upgrading in King's College London Active Surveillance cohort**. The area under the receiver operating characteristic curve or AUC (measure of discrimination) and mean absolute prediction error or MAPE (measure of calibration) are calculated over the follow-up period at a gap of 6 months. In addition bootstrapped 95% confidence intervals (CI) are also presented.

Follow-up period (years)	AUC (95% CI)	MAPE (95%CI)
0.0 to 1.0	0.589 [0.514, 0.653]	0.430 [0.407, 0.450]
0.5 to 1.5	0.660 [0.550, 0.742]	0.453 [0.431, 0.474]
1.0 to 2.0	0.683 [0.604, 0.753]	0.416 [0.396, 0.445]
1.5 to 2.5	0.691 [0.621, 0.766]	0.271 [0.246, 0.297]
2.0 to 3.0	0.689 [0.616, 0.785]	0.319 [0.282, 0.344]

Table 12: **External validation of predictions of upgrading in Michigan Urological Surgery Improvement Collaborative Active Surveillance cohort**. The area under the receiver operating characteristic curve or AUC (measure of discrimination) and mean absolute prediction error or MAPE (measure of calibration) are calculated over the follow-up period at a gap of 6 months. In addition bootstrapped 95% confidence intervals (CI) are also presented.

Follow-up period (years)	AUC (95% CI)	MAPE (95%CI)
0.0 to 1.0	0.639 [0.607, 0.672]	0.461 [0.450, 0.469]
0.5 to 1.5	0.617 [0.588, 0.652]	0.446 [0.441, 0.453]
1.0 to 2.0	0.599 [0.553, 0.632]	0.331 [0.317, 0.348]

Appendix C. Personalized Biopsies Based on Risk of Upgrading

Consider some real patients from the PRIAS database shown in Figure 9 to Figure 11. We intend to develop personalized schedule of biopsies for these patients. Using the joint model fitted to the PRIAS dataset, we first obtain their cumulative risk of upgrading over the entire follow-up period (see Equation 4, given their accumulated clinical data. Our aim is to employ this cumulative-risk function in the personalized biopsy schedule. However, in line with the protocols of most AS cohorts [12], we first schedule a compulsory biopsy at year one of follow-up. This promises early detection of Gleason upgrade for patients misdiagnosed as low-grade cancer patients, or patients who chose AS despite having a higher grade at diagnosis. We also maintain a recommended minimum gap of one year between consecutive biopsies [11]. Consequently, we schedule personalized biopsies starting from year two until year a maximum horizon (Table 13). The added benefit of this approach is that due to the longitudinal measurements accumulated over two years, and year one biopsy results, we are able to make reasonably accurate predictions of the cumulative-risk of Gleason upgrade.

We next exploit PRIAS cohort's fixed schedule of longitudinal measurements $L = \{2, 2.5 \dots 6\}$ between year two and six (horizon, Table 13). More specifically, we schedule a biopsy at all those future visits where the conditional cumulative-risk of Gleason upgrade is larger than a certain threshold $0 \leq \kappa \leq 1$ (e.g., 10% risk). The resulting personalized schedule of biopsies B_j^{κ} is given by:

$$B_j^{\kappa} = \Big\{ b_{jk} \epsilon L \mid R_j(b_{jk} \mid b_{jk-1}, s) \geq \kappa \wedge (b_{jk} - b_{jk-1} \geq 1) \Big\}, \tag{6}$$

where b_{jk} is the time of the k-th biopsy for the j-th patient. The conditional cumulative-risk of Gleason upgrade denoted by $R_j(b_{jk} \mid b_{jk-1}, s)$ is defined as in Equation (4). In this risk the contribution of the observed PSA $\mathcal{Y}_j(s)$ does not change while scheduling subsequent biopsies. However, the 'conditional' part here is that successive k-th biopsy at time b_{jk} is scheduled by accounting for the possibility that Gleason upgrade may not have occurred until the previously scheduled biopsy $T_j^* > b_{jk-1}$. The personalized schedule Equation (6) is updated as more patient data becomes available over follow-up.

To assist patients in making an informed choice for a schedule, be it personalized or fixed, we provide them patient-specific consequences of following each schedule. To this end, we first calculate the probability of occurrence of

Table 13: **Maximum follow-up period up to which we can reliably make personalized schedules**. In each cohort, this time point is chosen such that there are at least 10 patients who experience upgrading after this time point. Full names of Cohorts are *PRIAS*: Prostate Cancer International Active Surveillance, *Toronto*: University of Toronto Active Surveillance, *Hopkins*: Johns Hopkins Active Surveillance, *MSKCC*: Memorial Sloan Kettering Cancer Center Active Surveillance, *KCL*: King's College London Active Surveillance, *MUSIC*: Michigan Urological Surgery Improvement Collaborative Active Surveillance.

Cohort	Maximum Personalized Schedule Time (years)
PRIAS	6
KCL	3
MUSIC	2
Toronto	8
MSKCC	6
Hopkins	7

upgrading between successive biopsies of each schedule. Using these probabilities we then obtain the expected delay in detection of upgrading for following that schedule. Thus, patients have a method to compare across various schedules in terms of the personalized burden (time and total biopsies), and personalized benefit (less delay in detection of upgrading is beneficial). Suppose once again that for patient j, the time of latest negative biopsy is t_0, and current visit time is $s > t_0$. Then equation for the expected delay $D_j(B \mid t, s)$ in detection of upgrading using schedule of biopsies $B = \{t_1, \ldots, t_h\}$, where $t_1 \geq s$, and t_h is the horizon time (Table 13) up to which we want to schedule biopsies, is given by:

$$D_j(B \mid t, s) = \sum_{v=1}^{h} R_j(t_v \mid t_{v-1}, s) \times \Big\{ t_v - t_{v-1} - \int_{t_{v-1}}^{t_v} S_j(u \mid t_v, t_{v-1}, s) \mathrm{d}u \Big\},$$
$$S_j(u \mid t_v, t_{v-1}, s) = \Pr\big\{ T_j^* > u \mid t_v \geq T_j^* > t_{v-1}, \mathcal{Y}_j(s), \mathcal{D}_n \big\}, \quad t_v \geq u > t_{v-1}, \tag{7}$$

and $R_j(t_v \mid t_{v-1}, s)$ is as defined in Equation (4). The personalized and fixed schedules, and their consequences for a few real patients from the PRIAS dataset are shown in Figure 9 to Figure 11. A compulsory biopsy was done at horizon t_h of follow-up in all schedules for meaningful comparison of their expected delays in detection of upgrading.

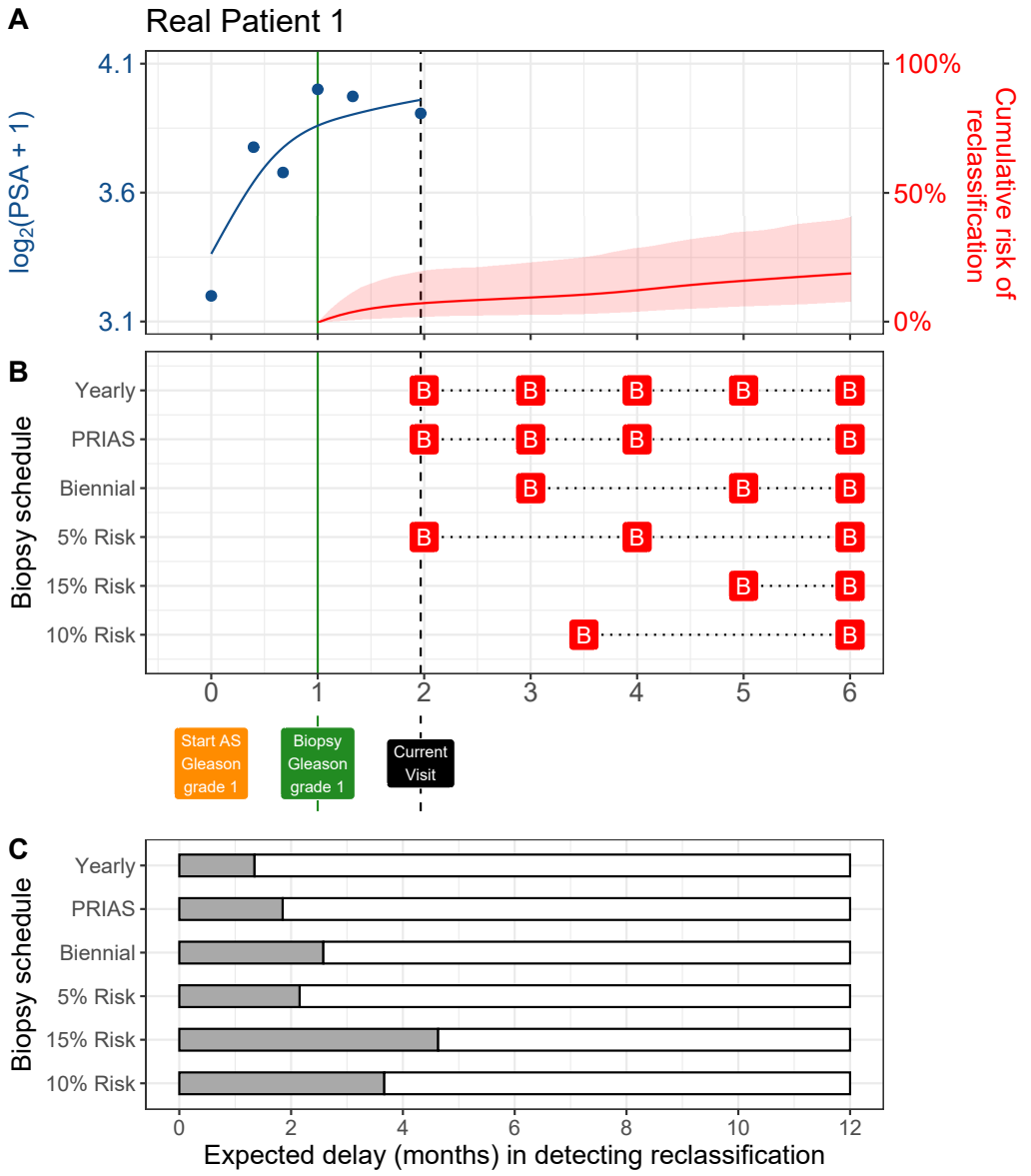

Figure 9: **Personalized and fixed schedules of biopsies for patient 1**. **Panel A:** shows the observed and fitted $\log_2(\text{PSA}+1)$ measurements (Equation 1), and the dynamic cumulative risk of upgrading (see Appendix B) over follow-up period. **Panel B** shows the personalized and fixed schedules of biopsies with a 'B' indicating times of biopsies. **Panel B** various schedules are compared in terms of the expected delay in detection of upgrading if they are followed.

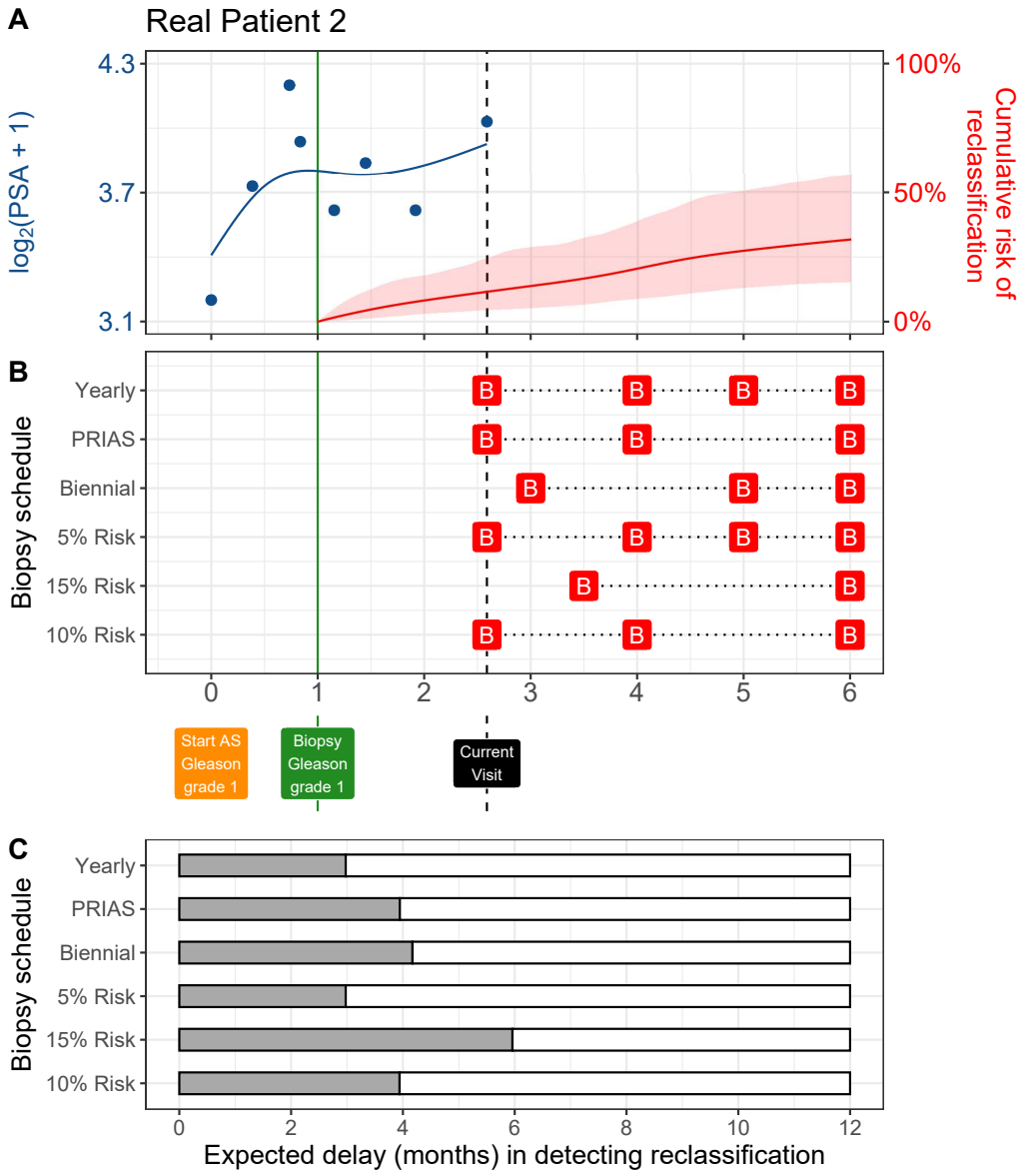

Figure 10: **Personalized and fixed schedules of biopsies for patient 2**. **Panel A:** shows the observed and fitted $\log_2(\text{PSA}+1)$ measurements (Equation 1), and the dynamic cumulative risk of upgrading (see Appendix B) over follow-up period. **Panel B** shows the personalized and fixed schedules of biopsies with a 'B' indicating times of biopsies. **Panel B** various schedules are compared in terms of the expected delay in detection of upgrading if they are followed.

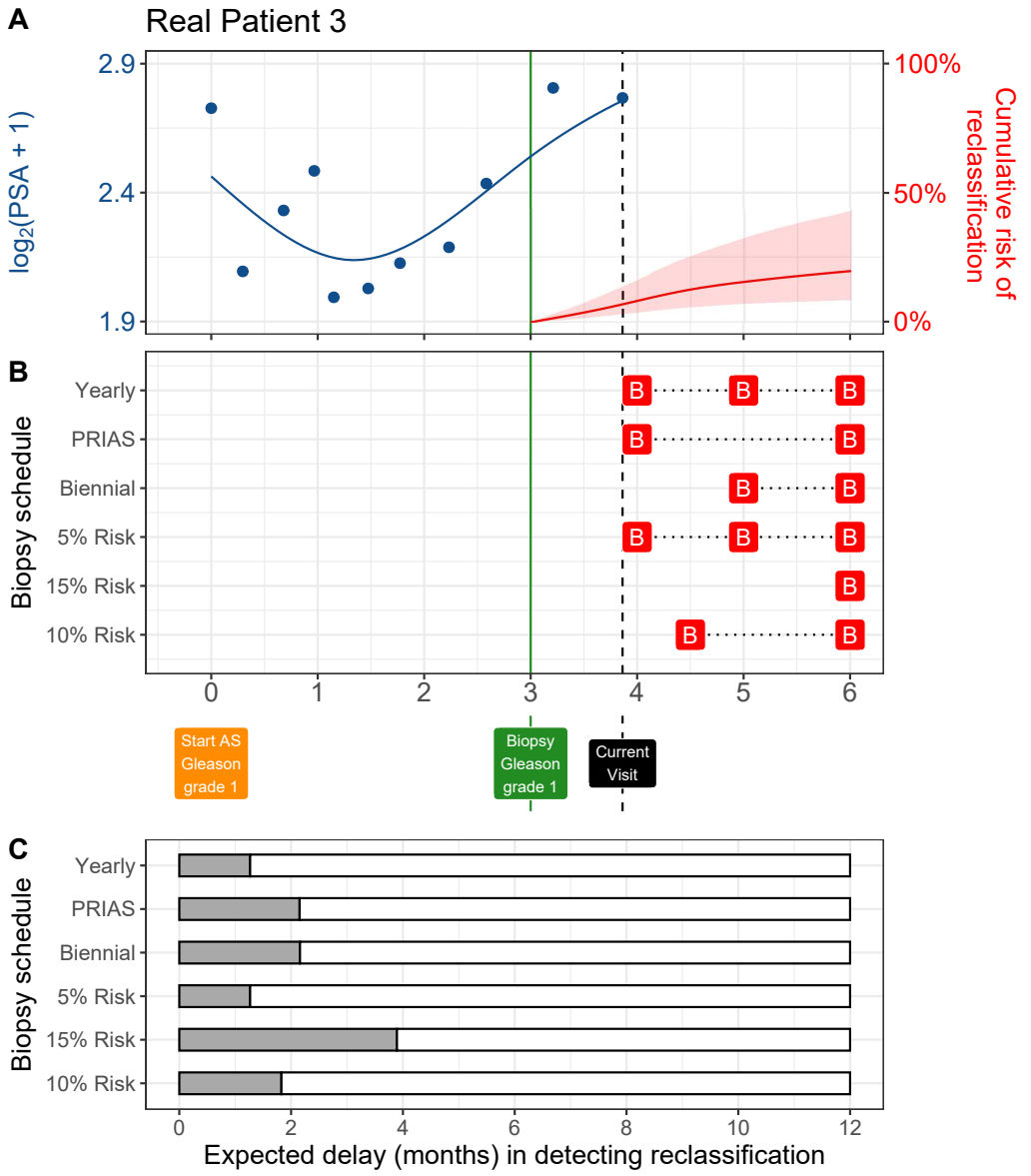

Figure 11: **Personalized and fixed schedules of biopsies for patient 3**. **Panel A:** shows the observed and fitted $\log_2(\text{PSA}+1)$ measurements (Equation 1), and the dynamic cumulative risk of upgrading (see Appendix B) over follow-up period. **Panel B** shows the personalized and fixed schedules of biopsies with a 'B' indicating times of biopsies. **Panel B** various schedules are compared in terms of the expected delay in detection of upgrading if they are followed.

Appendix D. Web Application for Practical Use of Personalized Schedule of Biopsies

We implemented our methodology in a web-application to assist patients and doctors in better decision making. It works on desktop as well as mobile devices. The cohorts that are currently supported in this web-application are PRIAS and the largest five cohorts from the GAP3 database [7]. These are the University of Toronto AS (Toronto), Johns Hopkins AS (Hopkins), Memorial Sloan Kettering Cancer Center AS (MSKCC), King's College London AS (KCL), and Michigan Urological Surgery Improvement Collaborative AS (MUSIC). The web-application is hosted at `https://emcbiostatistics.shinyapps.io/prias_biopsy_recommender/`.

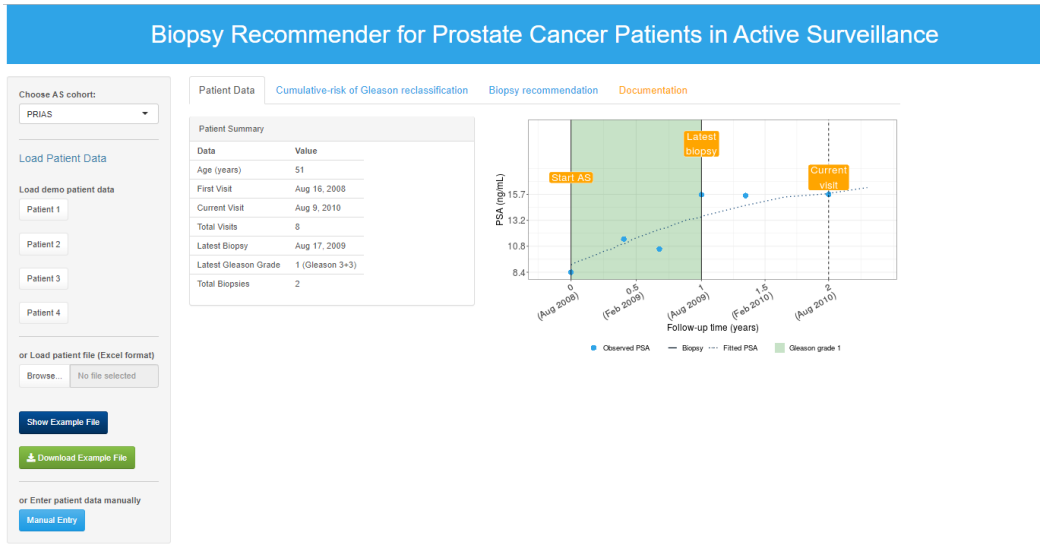

Figure 12: Landing page of the web-application. Panel on the left allows users to load patient data and panel on the right provides information. Patient data can be entered manually, or via Excel files. In addition, demo patient data is already uploaded to assist users in understanding the web-application.

Appendix E. Source Code

The R code for fitting the joint model to the PRIAS dataset, is at `https://github.com/anirudhtomer/prias/tree/master/src/clinical_gap3`. We refer to this location as 'R_HOME' in the rest of this document.

Appendix E.1. Fitting the Joint Model to the PRIAS dataset

Accessing the dataset: The PRIAS dataset is not openly accessible. However, access to the database can be requested via the contact links at `https://www.prias-project.org`.

Formatting the dataset: This dataset however is in the so-called wide format and also requires removal of incorrect entries. This can be done via the R script `R_HOME/dataset_cleaning.R`. This will lead to two R objects, namely 'prias_final.id' and 'prias_long_final'. The 'prias_final.id' object contains information about time of upgrading for PRIAS patients. The 'prias_long_final' object contains longitudinal PSA measurements, the time of biopsies and results of biopsies.

Fitting the joint model: We use a joint model for time to event and longitudinal data to model the evolution of PSA measurements over time, and to simultaneously model their association with the risk of upgrading. The R package we use for this purpose is called **JMbayes** (https://cran.r-project.org/web/packages/JMbayes/JMbayes.pdf). The API we use, however, are currently not hosted on CRAN, and can be found here: `https://github.com/anirudhtomer/JMbayes`. The joint model can be fitted via the script `R_HOME/analysis.R`. It takes roughly 6 hours to run on an Intel core-i5 machine with 4 cores, and 8GB of RAM.

The graphs presented in the main manuscript, and the supplementary material can be generated by the scripts in `R_HOME/plots/`.

Appendix E.2. Validation of Predictions of Upgrading

Validations can be done using the scripts `R_HOME/validation/auc_brier/auc_calculator.R`, and `R_HOME/validation/auc_brier/gof_calculator.R`. For external validation access to GAP3 database is required.

Appendix E.3. Creating Personalized Schedules of Biopsies

Once a joint model is fitted to the PRIAS dataset, personalized schedules of biopsies based on risk of upgrading for new patients can be developed using the script `R_HOME/scheduleCreator.R`. This script also provides fixed biopsy schedules for the patients. In addition with each schedule, the expected delay in detection of upgrading is also provided.

Appendix E.4. Source Code for Web Application

Source for the shiny web application which provides biopsy schedules for patients can be found at `R_HOME/shinyapp`

Appendix F. Appendix A. Members of The Movember Foundations Global Action Plan Prostate Cancer Active Surveillance (GAP3) consortium

Principle Investigators: Bruce Trock (Johns Hopkins University, The James Buchanan Brady Urological Institute, Baltimore, USA), Behfar Ehdaie (Memorial Sloan Kettering Cancer Center, New York, USA), Peter Carroll (University of California San Francisco, San Francisco, USA), Christopher Filson (Emory University School of Medicine, Winship Cancer Institute, Atlanta, USA), Jeri Kim / Christopher Logothetis (MD Anderson Cancer Centre, Houston, USA), Todd Morgan (University of Michigan and Michigan Urological Surgery Improvement Collaborative (MUSIC), Michigan, USA), Laurence Klotz (University of Toronto, Sunnybrook Health Sciences Centre, Toronto, Ontario, Canada), Tom Pickles (University of British Columbia, BC Cancer Agency, Vancouver, Canada), Eric Hyndman (University of Calgary, Southern Alberta Institute of Urology, Calgary, Canada), Caroline Moore (University College London & University College London Hospital Trust, London, UK), Vincent Gnanapragasam (University of Cambridge & Cambridge University Hospitals NHS Foundation Trust, Cambridge, UK), Mieke Van Hemelrijck (King's College London, London, UK & Guys and St Thomas NHS Foundation Trust, London, UK), Prokar Dasgupta (Guys and St Thomas NHS Foundation Trust, London, UK), Chris Bangma (Erasmus Medical Center, Rotterdam, The Netherlands/ representative of Prostate cancer Research International Active Surveillance (PRIAS) consortium), Monique Roobol (Erasmus Medical Center, Rotterdam, The Netherlands/ representative of Prostate cancer Research International Active Surveillance (PRIAS) consortium), Arnauld Villers (Lille University Hospital Center, Lille, France), Antti Rannikko (Helsinki University and Helsinki University Hospital, Helsinki, Finland), Riccardo Valdagni (Department of Oncology and Hemato-oncology, Universit degli Studi di Milano, Radiation Oncology 1 and Prostate Cancer Program, Fondazione IRCCS Istituto Nazionale dei Tumori, Milan, Italy), Antoinette Perry (University College Dublin, Dublin, Ireland), Jonas Hugosson (Sahlgrenska University Hospital, Gteborg, Sweden), Jose Rubio-Briones (Instituto Valenciano de Oncologa, Valencia, Spain), Anders Bjartell (Skne University Hospital, Malm, Sweden), Lukas Hefermehl (Kantonsspital Baden, Baden, Switzerland), Lee Lui Shiong (Singapore General Hospital, Singapore, Singapore), Mark Frydenberg (Monash Health; Monash University, Melbourne, Australia), Yoshiyuki

Kakehi / Mikio Sugimoto (Kagawa University Faculty of Medicine, Kagawa, Japan), Byung Ha Chung (Gangnam Severance Hospital, Yonsei University Health System, Seoul, Republic of Korea)

Pathologist: Theo van der Kwast (Princess Margaret Cancer Centre, Toronto, Canada). Technology Research Partners: Henk Obbink (Royal Philips, Eindhoven, the Netherlands), Wim van der Linden (Royal Philips, Eindhoven, the Netherlands), Tim Hulsen (Royal Philips, Eindhoven, the Netherlands), Cees de Jonge (Royal Philips, Eindhoven, the Netherlands).

Advisory Regional statisticians: Mike Kattan (Cleveland Clinic, Cleveland, Ohio, USA), Ji Xinge (Cleveland Clinic, Cleveland, Ohio, USA), Kenneth Muir (University of Manchester, Manchester, UK), Artitaya Lophatananon (University of Manchester, Manchester, UK), Michael Fahey (Epworth HealthCare, Melbourne, Australia), Ewout Steyerberg (Erasmus Medical Center, Rotterdam, The Netherlands), Daan Nieboer (Erasmus Medical Center, Rotterdam, The Netherlands); Liying Zhang (University of Toronto, Sunnybrook Health Sciences Centre, Toronto, Ontario, Canada)

Executive Regional statisticians: Ewout Steyerberg (Erasmus Medical Center, Rotterdam, The Netherlands), Daan Nieboer (Erasmus Medical Center, Rotterdam, The Netherlands); Kerri Beckmann (King's College London, London, UK & Guys and St Thomas NHS Foundation Trust, London, UK), Brian Denton (University of Michigan, Michigan, USA), Andrew Hayen (University of Technology Sydney, Australia), Paul Boutros (Ontario Institute of Cancer Research, Toronto, Ontario, Canada).

Clinical Research Partners IT Experts: Wei Guo (Johns Hopkins University, The James Buchanan Brady Urological Institute, Baltimore, USA), Nicole Benfante (Memorial Sloan Kettering Cancer Center, New York, USA), Janet Cowan (University of California San Francisco, San Francisco, USA), Dattatraya Patil (Emory University School of Medicine, Winship Cancer Institute, Atlanta, USA), Emily Tolosa (MD Anderson Cancer Centre, Houston, Texas, USA), Tae-Kyung Kim (University of Michigan and Michigan Urological Surgery Improvement Collaborative, Ann Arbor, Michigan, USA), Alexandre Mamedov (University of Toronto, Sunnybrook Health Sciences Centre, Toronto, Ontario, Canada), Vincent LaPointe (University of British Columbia, BC Cancer Agency, Vancouver, Canada), Trafford Crump (University of Calgary, Southern Alberta Institute of Urology, Calgary, Canada), Vasilis Stavrinides (University College London & University College London Hospital Trust, London, UK), Jenna Kimberly-Duffell (University of Cambridge & Cambridge University Hospitals NHS Foundation Trust, Cam-

bridge, UK), Aida Santaolalla (King's College London, London, UK & Guys and St Thomas NHS Foundation Trust, London, UK), Daan Nieboer (Erasmus Medical Center, Rotterdam, The Netherlands), Jonathan Olivier (Lille University Hospital Center, Lille, France), Tiziana Rancati (Fondazione IRCCS Istituto Nazionale dei Tumori di Milano, Milan, Italy), Heln Ahlgren (Sahlgrenska University Hospital, Gteborg, Sweden), Juanma Mascars (Instituto Valenciano de Oncologa, Valencia, Spain), Annica Lfgren (Skne University Hospital, Malm, Sweden), Kurt Lehmann (Kantonsspital Baden, Baden, Switzerland), Catherine Han Lin (Monash University and Epworth HealthCare, Melbourne, Australia), Hiromi Hirama (Kagawa University, Kagawa, Japan), Kwang Suk Lee (Yonsei University College of Medicine, Gangnam Severance Hospital, Seoul, Korea).

Research Advisory Committee: Guido Jenster (Erasmus MC, Rotterdam, the Netherlands), Anssi Auvinen (University of Tampere, Tampere, Finland), Anders Bjartell (Skne University Hospital, Malm, Sweden), Masoom Haider (University of Toronto, Toronto, Canada), Kees van Bochove (The Hyve B.V. Utrecht, Utrecht, the Netherlands), Ballentine Carter (Johns Hopkins University, Baltimore, USA until 2018).

Management team: Sam Gledhill (Movember Foundation, Melbourne, Australia), Mark Buzza / Michelle Kouspou (Movember Foundation, Melbourne, Australia), Chris Bangma (Erasmus Medical Center, Rotterdam, The Netherlands), Monique Roobol (Erasmus Medical Center, Rotterdam, The Netherlands), Sophie Bruinsma / Jozien Helleman (Erasmus Medical Center, Rotterdam, The Netherlands).

References

1. Epstein JI, Egevad L, Amin MB, Delahunt B, Srigley JR, Humphrey PA. The 2014 international society of urological pathology (isup) consensus conference on gleason grading of prostatic carcinoma. *The American journal of surgical pathology* 2016;40(2):244–52.

2. Pearson JD, Morrell CH, Landis PK, Carter HB, Brant LJ. Mixed-effects regression models for studying the natural history of prostate disease. *Statistics in Medicine* 1994;13(5-7):587–601.

3. Lin H, McCulloch CE, Turnbull BW, Slate EH, Clark LC. A latent class mixed model for analysing biomarker trajectories with irregularly scheduled observations. *Statistics in Medicine* 2000;19(10):1303–18.

4. De Boor C. A practical guide to splines; vol. 27. Springer-Verlag New York; 1978.

5. Eilers PH, Marx BD. Flexible smoothing with B-splines and penalties. *Statistical Science* 1996;11(2):89–121.

6. Turnbull BW. The empirical distribution function with arbitrarily grouped, censored and truncated data. *Journal of the Royal Statistical Society Series B (Methodological)* 1976;38(3):290–5.

7. Bruinsma SM, Zhang L, Roobol MJ, Bangma CH, Steyerberg EW, Nieboer D, Van Hemelrijck M, consortium MFGAPPCASG, Trock B, Ehdaie B, et al. The movember foundation's gap3 cohort: a profile of the largest global prostate cancer active surveillance database to date. *BJU international* 2018;121(5):737–44.

8. Rizopoulos D. The R package JMbayes for fitting joint models for longitudinal and time-to-event data using MCMC. *Journal of Statistical Software* 2016;72(7):1–46.

9. Rizopoulos D, Molenberghs G, Lesaffre EM. Dynamic predictions with time-dependent covariates in survival analysis using joint modeling and landmarking. *Biometrical Journal* 2017;59(6):1261–76.

10. Steyerberg EW, Vickers AJ, Cook NR, Gerds T, Gonen M, Obuchowski N, Pencina MJ, Kattan MW. Assessing the performance of prediction models: a framework for some traditional and novel measures. *Epidemiology (Cambridge, Mass)* 2010;21(1):128.

11. Bokhorst LP, Alberts AR, Rannikko A, Valdagni R, Pickles T, Kakehi Y, Bangma CH, Roobol MJ, PRIAS study group . Compliance rates with the Prostate Cancer Research International Active Surveillance (PRIAS) protocol and disease reclassification in noncompliers. *European Urology* 2015;68(5):814–21.

12. Nieboer D, Tomer A, Rizopoulos D, Roobol MJ, Steyerberg EW. Active surveillance: a review of risk-based, dynamic monitoring. *Translational andrology and urology* 2018;7(1):106–15.